UDC 541.64:574.24:553.08

The Methods of non-equilibrium Spectrum (NES) and Differential non-equilibrium Spectrum (DNES) in Studying the Interaction of Carbonaceous Mineral Shungite and Aluminosilicate Mineral Zeolite with Water

[1] Ignat Ignatov
[2] Oleg Mosin

[1] The Scientific Research Center of Medical Biophysics (SRC MB), Bulgaria
Professor, D. Sc., director of SRC MB
1111, Sofia, N. Kopernik street, 32
E-mail: mbioph@dir.bg
[2] Moscow State University of Applied Biotechnology, Russian Federation
Senior research Fellow of Biotechnology Department, Ph. D. (Chemistry)
103316, Moscow, Talalihina ulitza, 33
E-mail: mosin-oleg@yandex.ru

Abstract

The mathematical model of interaction with water the amorphous, uncrystallized, fullerene analogous carbon containing natural mineral shungite (Zazhoginskoe deposit, Karelia, Russia) and micro-porous alumosilicate mineral zeolite (Most, Bulgaria) was established. There are submitted data on the nanostructure and structural properties of these minerals, obtained with using the elemental analysis, transmission electron microscopy (TEM-method) and IR-spectroscopy. For evaluation of the mathematical model of interaction of these minerals with water, the methods of non-equilibrium spectrum (NES) and differential non-equilibrium spectrum (DNES) of water were applied. The values of average energy ($\Delta E_{H...O}$) of hydrogen H...O-bonds among H_2O molecules in water samples after the treatment of shungite and zeolite with water was measured at -0,1137 eV for shungite and -0,1174 eV for zeolite. The calculation of $\Delta E_{H...O}$ for shungite with using the DNES method compiles +0,0025±0,0011 eV and for zeolite -1,2±0,0011 eV. It was demonstrated a regularity of change of energy of hydrogen bonds between H_2O molecules in the process of water treatment by shungite and zeolite with a statistically reliable increase of local maximums in DNES-spectra.

Keywords: shungite, zeolite, nanostructure, fullerens, IR, NES, DNES

Introduction

Shungite and zeolite – the minerals refer to new generation of natural mineral sorbents (NMS). Shungite is an intermediate form between the amorphous carbon and the graphite crystal, containing carbon (30 %), silica (45 %), and silicate mica (about 20 %) [1]. The schungite carbon is a fossilized organic material of the sea bottom Precambrian sediments of high level of carbonization containing the fullerene-like regular structures. Shungite got its name after the village of Shunga in Karelia (Russian Federation), located on the shore of Onezhskoe Lake, where is

located the only one mineral Zazhoginsky deposit of shungites on the territoty of the Russian Federation. The total shungite researves of Zazhoginsky deposit amount to approximately 35 million tons of shungite. The plant production capacity for the mining and processing of shungite makes up 200 thousand tons of shungite per year.

Zeolites are the alumosilicate members of the family of microporous solids known as "molecular sieves", named by their ability to selectively sort molecules based primarily on a size exclusion process. The natural zeolites formed when the volcanic rocks and ash layers reacted with alkaline groundwater. Zeolites also crystallize in post-depositional environments over periods ranging from thousands to millions of years in shallow marine basins. The naturally occurring zeolites are rarely pure and are contaminated to varying degrees by other minerals, metals, quarts, or other zeolites. For this reason, naturally occurring zeolites are excluded from many important commercial applications where uniformity and purity are essential.

As natural minerales shungite and zeolite have unusually broad scope of application in industry. Shungite was used initially, mainly as a filler and substitute of the carbon coal coke (fuel) in blast furnace production of high-silicon cast iron, in ferroalloys melting, in the production of non-stick heat-resistant paints and coatings, and as filler in rubber production. Subsequently there were discovered other new valuable properties of shungite – adsorptional, bactericidal, catalytic, reduction-oxidation properties, as well as the ability of sungite minerals to screen off electromagnetic and radio radiations. These properties have made the use of shungite in various branches of science, industry and technology, for creating on its basis a variety of new nanotechnological materials with nano-molecular structure [2]. On the basis of shuntite has been created new conductive paints, fillers for plastic materials, rubber and carbon black substitutes, composite materials, concrete, bricks, stuccoing plasters, asphalts, as well as materials having bactericidal activity and materials shilding off the radio and electromagnetic radiation. The adsorption, catalytic, and reduction-oxydation properties of shungite favored its use in water treatment and water purification technologies [3], i.g. in treatment of sewage waters from many organic and inorganic substances (heavy metals, ammonia, organochlorine compounds, petroleum, phenols, surfactants, etc.). Moreover, shungite has a strongly marked biological activity and bactericidal properties.

Zeolites as shungites are widely used in industry as a desiccant of gases and liquids [4], for treatment of drinking and sewage water from heavy metals, ammonia, phosphorus [5], as a catalyst in petrochemical industry (shungite), for benzene extraction and for extracting of radionuclides in nuclear reprocessing. They are also used in medicine as nutritional supplements having antioxidant properties.

A wide range of properties of shungite and zeolite defines the search for new areas of industrial application of these minerals in science and technology that contributes to a deeper study of the structure with using the modern analytical methods. This research paper deals with investigation of the structural properties of shungite and zeolite and evaluation of the mathematical model of interaction of these minerals with water.

Material and methods
Material
The study was performed with samples of shungite obtained from Zazhoginsky deposit (Karelia, Russia) and zeolite (Most, Bulgaria). Samples were taken and analyzed in solid samples according to National standard of the Russian Federal Agency of Technical Regulation and Metrology. Samples were put into 100 cm^3 hermetically sealed glass tubes after being washed in dist. H_2O and dried in crucible furnace, and homogenized in homogenizer by mechanical grinding. For the decomposition of the shungite samples a system of microwave decomposition was used. Other methods of samples processing were watching with dist. H_2O, drying, and homogenization on cross beater mill Retsch SK100 ("Retsch Co.", Germany) and Pulverisette 16 ("Fritsch GMBH", Germany).

Analytical methods
The analytical methods were accredited by the Institute of Geology of Ore Deposits, Petrography, Mineralogy, and Geochemistry (Russian Academy of Sciences). Samples were treated by various methods as ICP-OES, GC, and SEM.

Gas-chromatography

Gas-chromatography (GC) was performed at Main Testing Centre of Drinking Water (Moscow, the Russian Federation) on Kristall 4000 LUX M using Chromaton AW-DMCS and Inerton-DMCS columns (stationary phases 5 % SE-30 and 5 % OV-17), equipped with flame ionization detector (FID) and using helium (He) as a carrier gas.

Inductively coupled plasma optical emission spectrometry (ICP-OES)

The mineral composition of shungite was studied by inductively coupled plasma optical emission spectrometry (ICP-OES) on Agilent ICP 710-OES (Agilent Technologies, USA) spectrometer, equipped with plasma atomizer (under argon stream), Mega Pixel CCD detector, and 40 MHz free-running, air-cooled RF generator, and Computer-optimized echelle system: the spectral range at 167–785 nm; plasma gas: 0–22,5 l/min in 1,5 l/min; power output: 700–1500 W in 50 W increments.

Elemental analysis

The total amount of carbon (C_{total}) in shungite was measured according to the ISO 29541 standard using elemental analyzer CHS-580 ("Eltra GmbH", Germany), equipped with electric furnace and IR-detector by combustion of 200 mg of solid homogenized sample in a stream of oxygen at the temperature +1500 ^{0}C.

Transmission electron microscopy

The structural studies were carried out with using transmission electron microscopy (TEM) on JSM 35 CF (JEOL Ltd., Korea) device, equipped with X-ray microanalyzer "Tracor Northern TN", SE detector, thermomolecular pump, and tungsten electron gun (Harpin type W filament, DC heating); working pressure: 10^{-4} Pa (10^{-6} Torr); magnification: 300000, resolution: 3,0 nm, accelerating voltage: 1–30 kV; sample size: 60–130 mm.

IR-spectroscopy

IR-spectra of shungite were registered on Fourier-IR spectrometer Brucker Vertex ("Brucker", Germany) (a spectral range: average IR – 370–7800 cm^{-1}; visible – 2500–8000 cm^{-1}; the permission – 0,5 cm^{-1}; accuracy of wave number – 0,1 cm^{-1} on 2000 cm^{-1}).

NES- and DNES-methods

NES- and DNES-methods were used for the estimation of energy of hydrogen bonds of shungite zeolite solutions in water in order to evaluate the mathematical model of interaction of these minerals with water. The device measured the angle of evaporation of water drops from 72^0 to 0^0. As the main estimation criterion was used the average energy ($\Delta E_{H...O}$) of hydrogen O...H-bonds between individual H_2O molecules in aqueous samples. NES-and DNES spectra of shungite and zeolite solutions in water were measured in the range of the energy of hydrogen bonds 0,08–0,387 eV or wave lengths λ = 8,9–13,8 μm with using a specially designed computer program.

Results and Discussion
The composition and the structure of shungite and zeolite

According to the last structural studies shungite is a metastable allotropic form of carbon with high level of carbonization (carbon metamorhism), being on prior to graphite stage of coalification [6]. Along with carbon the shungite, obtained from Zazhoginsky deposit in Karelia (Russian Federation) contains SiO_2 (57,0 %), TiO_2 (0,2 %), Al_2O_3 (4,0 %), FeO (0,6 %), Fe_2O_3 (1,49 %), MgO (1,2 %), MnO (0,15 %), K_2O (1,5 %), S (1,2 %) (Table 1). The product obtained after the thermal firing of shungite (shungizite) at +1200...+1400 ^{0}C contains in small amounts V (0,015 %),

B (0,004 %), Ni (0,0085 %), Mo (0,0031 %), Cu (0,0037 %), Zn (0,0067 %), Co (0,00014 %) As (0,00035 %), Cr (0,72 %), Zn (0,0076 %) and other elements (Table 2).

Table 1: The chemical composition of shungites from Zazhoginsky deposit (Karelia, Russian Federation), in % (w/w)

| №	Chemical component	Content, % (w/w)
1	C	30,0
2	SiO_2	57,0
3	TiO_2	0,2
4	Al_2O_3	4,0
5	FeO	0,6
6	Fe_2O_3	1,49
7	MgO	1,2
8	MnO	0,15
9	CaO	0,3
10	Na_2O	0,2
11	K_2O	1,5
12	S	1,2
13	H_2O	1,7

Table 2: The chemical composition of shungite after the heat treatment at +1400 ⁰C

№	Chemical component	Content, % (w/w)
1	C	26,25
2	SiO_2	3,45
3	TiO_2	0,24
4	Al_2O_3	3,05
5	FeO	0,32
6	Fe_2O_3	1,01
7	MgO	0,56
8	MnO	0,12
9	CaO	0,12
10	Na_2O	0,36
11	K_2O	1,23
12	S	0,37
14	P_2O_3	0,03
15	Ba	0,32
16	B	0,004
17	V	0,015
18	Co	0,00014
19	Cu	0,0037
20	Mo	0,0031
21	As	0,00035
22	Ni	0,0085
23	Pb	0,0225
24	Sr	0,001
26	Cr	0,0072
26	Zn	0,0067
27	H_2O	0,78
28	Calcination (burning) losses	32,78

In comparison with shungite, zeolite comprises a microporous crystalline aluminosilicate mineral commonly used as a commercial adsorber, the three-dimensional framework of which is

formed by the tetrahedra – $[AlO_4]^{2-}$ and $[SiO_4]^{2-}$ linking to each other via the vertices [7]. Each tetrahedron $[AlO_4]^{2-}$ creates a negative charge of the carcasses compensated by cations (H^+, Na^+, K^+, Ca^{2+}, NH_4^+, etc.), which in most cases capable of cation exchange in water solutions. In between the crystalline framework are arranged the hydrated positive ions of alkali and alkaline earth metals – sodium, potassium, calcium, less magnesium, barium, strontium, compensating the carcass charge and water molecules. The tetrahedrons $[AlO_4]^{2-}$ and $[SiO_4]^{2-}$ form the secondary structural units, such as six-membered rings, five-membered rings, truncated octahedra, etc. (Fig. 1). As a result the zeolite framework composes the interacting channels and cavities forming a porous structure with a pore size of 0,3–1,0 nm. An average crystal size of the zeolite may range from 0,5 to 30 µm.

The empirical formula of zeolite can be represented as follows:

$$M_{2/n}O \cdot Al_2O_3 \cdot \gamma SiO_2 \cdot wH_2O,$$
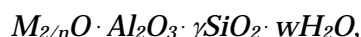
where n – the cationic charge ($n = 1$–2); γ – the molar ratio of oxides of silicon and aluminum in the zeolite framework, indicating the amount of cation exchange positions in the structure ($y = 2$–∞); w – the amount of water.
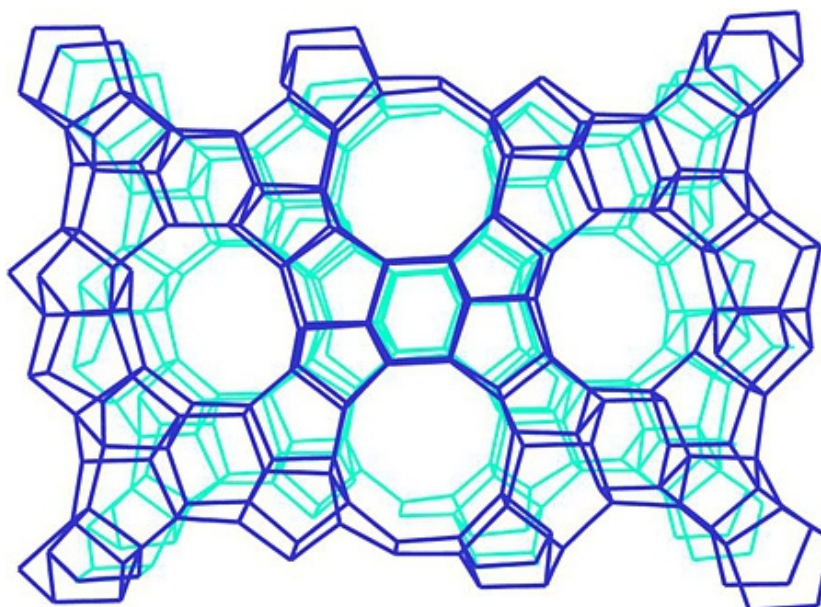

Figure 1. The three-dimensional crystal structure of zeolite ZSM-5 with the formula $Na_2[Al_2Si_{96-n}O_{192}] \cdot 16H_2O$ (n = 3–5), cell size − 0,51–0,56

Currently, there are known more than 30 varieties of natural zeolites, but only some of them form large deposits (80 % of concentrates) suitable for industrial processing. The most common natural zeolites:

• Chabazite $(Ca,Na_2)[Al_2Si_4O_{12}] \cdot 6H_2O$ with cell size 0,37–0,50 nm;
• Mordenite $(Ca,Na_2,K_2)[Al_2Si_{10}O_{24}] \cdot 7H_2O$ with cell size 0,67–0,70 nm;
• Klinoptilomite $(Na_2,K_2,Ca)[Al_2O_3 \cdot 10SiO_2] \cdot 8H_2O$ with cell size 0,75–0,82 nm.

The synthetic zeolites have the composition and the crystal structure similar to the natural zeolites:

• Zeolites of A-type A are represended by low silicate forms: in them the ratio $SiO_2:Al_2O_3$ does not exceed 2,0;
• Zeolites of X-type have the ratio $SiO_2:Al_2O_3$, which varies from 2,2 to 3,3;
• Zeolites of Y-type are characterized by the ratio of $SiO_2:Al_2O_3$ in the range of 3,1 to 6,0. By increasing this ratio the acid resistance of zeolites increases. The pore sizes define the selectivity which varies from 0,0003 to 0,0009 µm.

The composition of zeolite from Most (Bulgaria) is analogous to that of shungite (Table 3), except for carbon which does not occur in zeolite. The amounts of core elements (SiO_2, TiO_2, Al_2O_3, FeO, Fe_2O_3, MgO, CaO, Na_2O, K_2O, S) constituting this mineral differ from that of shungite: their content is higher than that of shungite, except for TiO_2 and K_2O, the contents of which in zeolite were dicreased (Table 3). The content of microelements as V (0,0272 %), Co (0,0045 %), Cu (0,0151 %), Mo (0,0012 %), As (0,0025 %), Ni (0,0079 %), Zn (0,1007 %), Zn (0,1007 %) was somewhat increased in zeolite, while the content of Ba (0,0066 %) and Cr (0,0048 %) was increased (Table 3).

Table 3: The chemical composition of zeolite (Most, Bulgaria), in % (w/w)

№	Chemical component	Content, % (w/w)
1	SiO_2	22,14
2	TiO_2	0,01
3	Al_2O_3	17,98
4	FeO	23,72
5	Fe_2O_3	1,49
6	MgO	14,38
7	MnO	0,61
8	CaO	0,36
9	Na_2O	0,5
10	K_2O	0,4
11	S	0,32
12	P_2O_5	0,06
13	Ba	0,0066
14	V	0,0272
15	Co	0,0045
17	Cu	0,0151
18	Mo	0,0012
19	As	0,0025
20	Ni	0,0079
21	Pb	0,0249
22	Sr	0,0021
23	Cr	0,0048
24	Zn	0,1007
25	H_2O	1,43

The physical and chemical properties of shungite and zeolite have been sufficiently studied [8]. The density of shungite makes up 2,1–2,4 g/cm^3; the porosity – up to 5 %; the compressive strength – 1000–1200 kgf/cm^2; the conductivity coefficient – 1500 SI/m; the thermal conductivity coefficient – 3,8 W/m·K, the adsorption capacity – up to 20 m^2/g. The density of zeolite – 1,7–2,1 g/cm^3; the porosity – 50 %; the adsorption capacity is 5 m^2/g; an average pore size – 0,4–0,6 nm.

Shungites differ in composition of their mineral matrix (aluminosilicate, siliceous, carbonate), and the amount of carbon in schungite samples. The shungite minerals with silicate mineral basis are divided into the low-carbon (5 % C), medium-carbon (5–25 % C), and high-carbon schungites (25–80 % C) [9]. The sum of (C + Si) in shungites of the Zazhoginsky deposit (Karelia, Russian Federation) generally is varied within 83–88 % as shown in Figure 2. The molar ratios of SiO_2 and Al_2O_3 in the aluminosilicate framework of the zeolite comprise ~2–3 units.
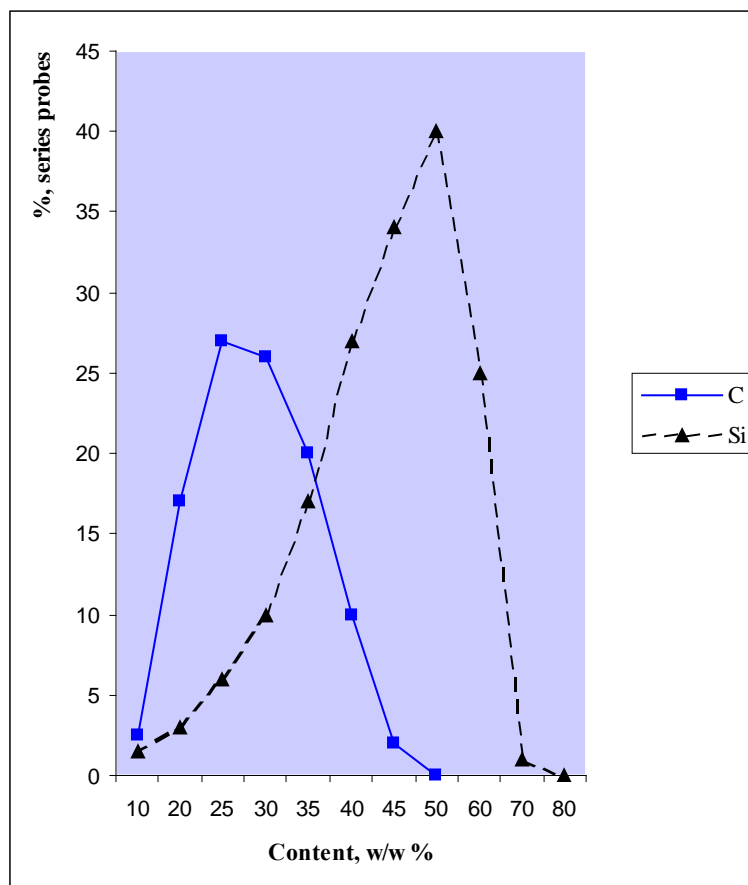
Figure 2. The distribution (%) of carbon (C) (solid line) and silicon (Si) (dotted line) in shungate samples from Zazhoginsky deposit (Karelia, Russian Federation) according to atomic emission spectrometry (AES)

The crystals of the crushed, fine ground shungite possess strong bipolar properties. This results in a high adhesion, and the ability of shungite to mix up with almost all organic and inorganic substances. Besides, shungite has a broad spectrum of bacterecidal properties; the mineral is the actively adsorptive against some bacterial cells, phages, and pathogenic saprophytes [10].

The unique properties of the mineral are defined by the nanostructure and composition of its constituent elements. The schungite carbon is equally distributed in the silicate framework of fine dispersed quartz crystals having the size of 1–10 μm [11, 12], as was confirmed by the studying of ultra-thin sections of shungite by transmission electron microscopy (TEM) in absorbed and backscattered electrons (Fig. 3).
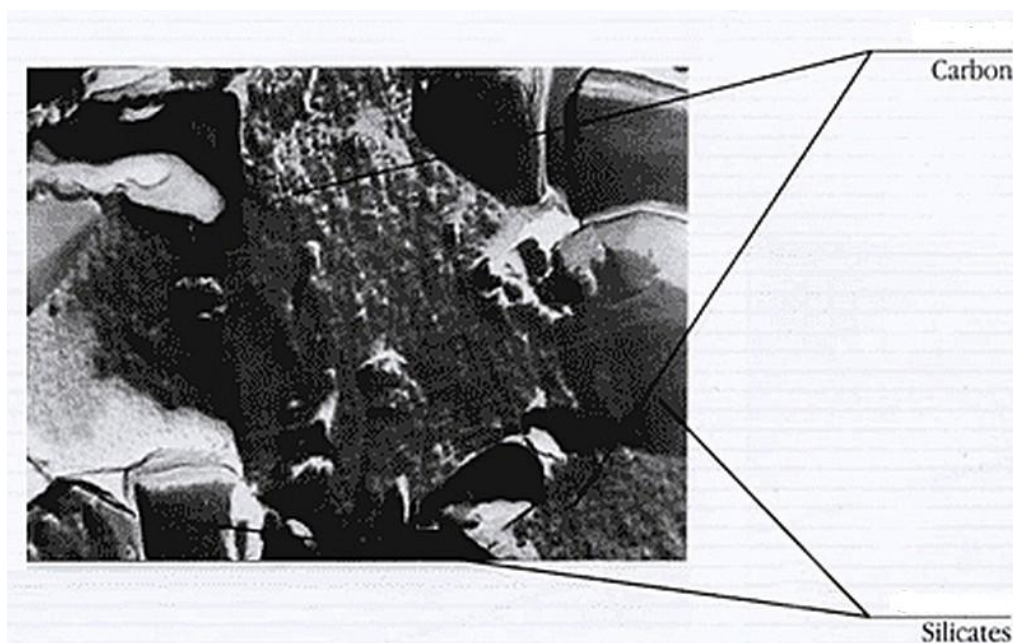
Figure 3. Structure of schungite rock obtained by the TEM method [11]. Scanning area 100×100 mm, resolution 0,5 nm, magnification 300000 times. The arrows show the silicate framework of fine dispersed quartz with the size 1–10 μm, and uniformly distributed carbon

The carbonaceous material of shungite is the product of a high degree of carbonization of hydrocarbons. Its elemental composition (%, w/w): C – 98,6–99,6; H – 0,15–0,5; (H + O) – 0,15–0,9 [13]. With virtually constant elemental composition of shungite, the carbonaceous matter is demonstrated the variability in its structure – both molecular and supramolecular, as well as surface, and porous structure. X-ray studies showed that the molecular structure of schungite carbon is represented by a solid uncristallized carbon, which components may have been in a state close as to the graphite and the carbon black and the glassy carbon as well, i.e. the maximally disordered [14]. The carbonaceous matter of shungite having a strongly marked structural anisotropy shows a significant increase in the diamagnetism at low temperatures that is a characteristic feature for fullerites [15].

The basis of the shungite carbon compose the hollow carbon fullerene-like multilayer spherical globules with a diameter of 10–30 nm, comprizing inclusive packages of smoothly curved carbon layers covering the nanopores (Fig. 4). The globule structure is stable relative to the shungite carbon phase transitions into other allotropic carbon forms. The fullerene-like globules (the content of fullerenes makes up ~0,001 %) may contain from a few dozen to a several hundred carbon atoms and may vary in shape and size [16].
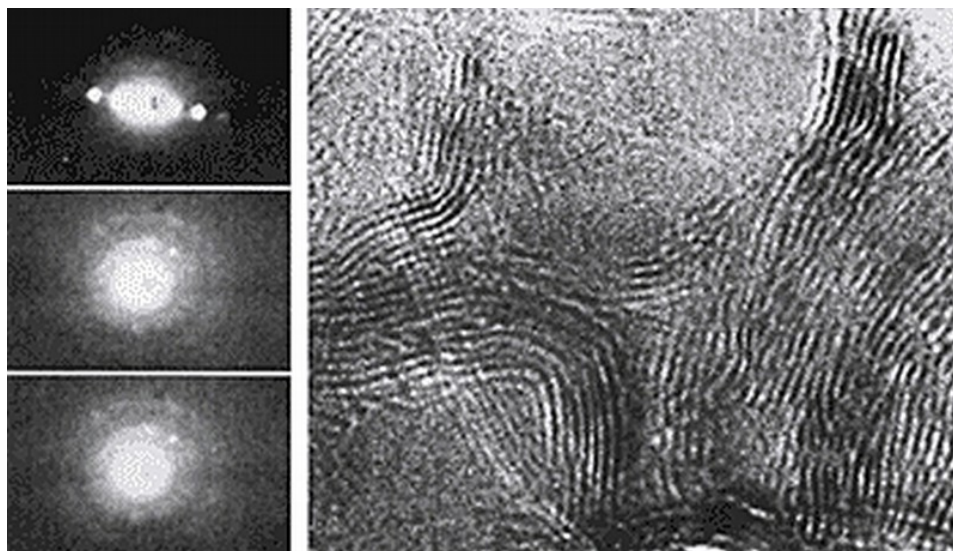
Figure 4. Electron diffraction of nanopattern of shungite carbon in the form of spherical multilayer fullerene globules with a diameter 10–30 nm, obtained by the TEM method [14] (the probe size 0,5–0,7 nm, the energy of the electron beam 100–200 kV, the beam radius 10 nm, the range of the goniometer rotation -27⁰...+27 ⁰). On the left are shown fluoresent spherical fullerene-like globules, on the right – the multi-layered spherical fullerene-like globules with packets of carbon layers, recorded at a higher resolution

Moreover, the carbonaceous matter of shungite has structural anisotropy and shows a significant increase of diamagnetism at low temperatures characteristic to the crystals formed by fullerene molecules (fullerites) [17]. Fullerites are molecular crystals with a faced-centered cubic (FCC) lattice size of 1,42 nm, the number of nearest neighbors – 12 and the distance between them – 1 nm. The density of fullerite is 1,7 g/cm³, which is slightly lower than the density and shungite (2,1–2,4 g/cm³), and graphite (2,3 g/cm³). Fullerene molecules may comprise 24, 28, 32, 36, 50, 60, 70, etc. carbon atoms (Fig. 5). Fullerenes with the number of carbon atoms n < 60 are unstable. Higher fullerenes containing more carbon atoms (n < 400) are produced in small quantities and often have rather difficult isomer composition [18]. The carbonaceous material of shungite in its composition contains fullerenes (C60, C70, C74, C76, C84, etc.), and fullerene-like structures, as separate and as well as related with minerals [19].
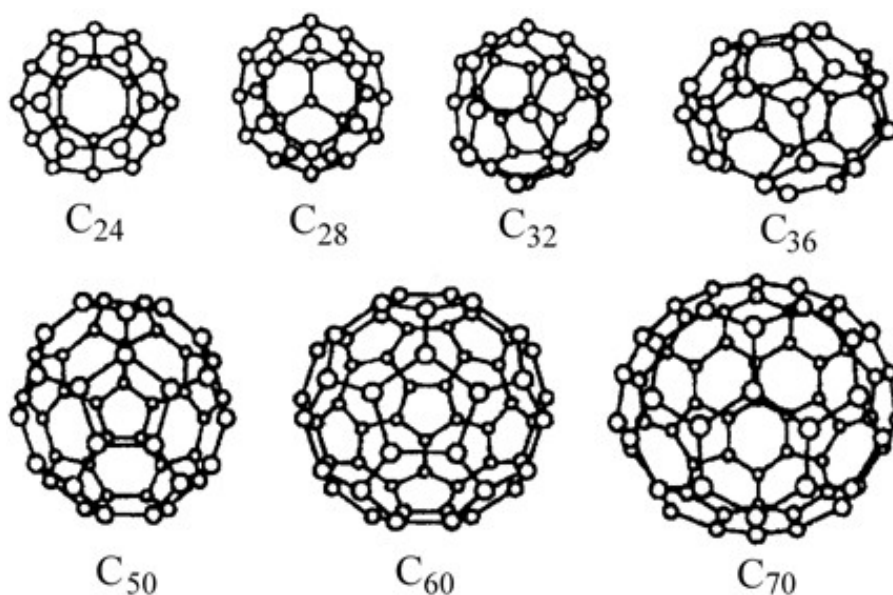

Figure 5. Varieties of fullerenes found in natural shungite with different numbers of carbon atoms: C24, C28, C32, C36, C50, C60, C70

Currently, the research is underway to modify the natural shungites to produce a mixed nanocarbon materials and increase the aggregate stability of the carbon nanoparticles in aqueous colloidal solutions of shungites and fullerenes [20]. It is also being discussed the idea of creating a drug carriers based on water-soluble endohedral fullerene compounds and natural fullerene material in which is placed inside one or more atoms of an element with radioactive isotopes. The conditions of synthesis of antiviral and anticancer drugs based on fullerenes, which introduction into the body allow a selective impact on the affected cancer cells, thus preventing their further reproduction. The prospects of development of the fullerene synthesis associated with the peculiarities of the chemical structure of fullerene molecules – the three dimensional analogues of aromatic structures and the presence of a large number of double conjugated bonds and reaction centers on a closed carbon sphere. Fullerenes having the high electronegativity, act in chemical reactions as a strong oxidizing agents. By allying to itself the radicals of different chemical nature, fullerenes can form a wide class of chemical compounds having different physico-chemical properties. At the present time it was synthesized about 3 thousand compounds based on fullerenes.

IR-studies of shungite

A convenient method to obtain information on the composition and the structure of a mineral is IR spectroscopy. IR spectra can usually be obtained with the amount of 0,5–3,0 mg of the sample, i.e. significantly less than required for NMR. In contrast to the NMR the measuring of IR-spectra is possible for solid compounds, which allows the study even insoluble solid substances.

By the method of IR-spectroscopy in the range of vibrations in the crystal mineral framework it is possible to obtain the information:

a) on the composition of the mineral and its components;

b) on the structure of the framework, particularly the lattice ratio type C/SiO_2 or SiO_2/Al_2O_3;

c) on the nature of the surface of the structural groups, which often serve as adsorption and catalytically active sites.

The wave absorption in the infrared region (400–4000 nm) is caused by the vibrational motion of the molecules associated with changes in bond lengths (stretching vibrations, ν) or bond angles between the atoms (deformation vibrations, δ). The IR spectrum of the carbon containing organic compound ranges from 400–4000 cm^{-1} and allows identify these compounds. However, often the interpretation of natural carbon-containing minerals is difficult due to their multi-component composition and as the result numerous oscillations in samples. Furthermore, the number of absorption bands in the IR spectra may differ from the number of normal molecular vibrations due to the occurrence of additional bands: overtones, component frequencies, and overlapping lines due to the Fermi resonance.

The research of shungite with using the method of IR-spectroscopy revealed the presence at least seven main maxima in the IR-spectrum of shungite, detected at 2,90; 3,18; 3,32; 6,13; 7,14; 8,59; 9,21 μm (wave length, λ), or 3448; 3141; 3016; 1630; 1400; 1164 and 1086 cm^{-1} (wave number, k) corresponding to oscillations of various organic group types in shungite (Fig. 6).
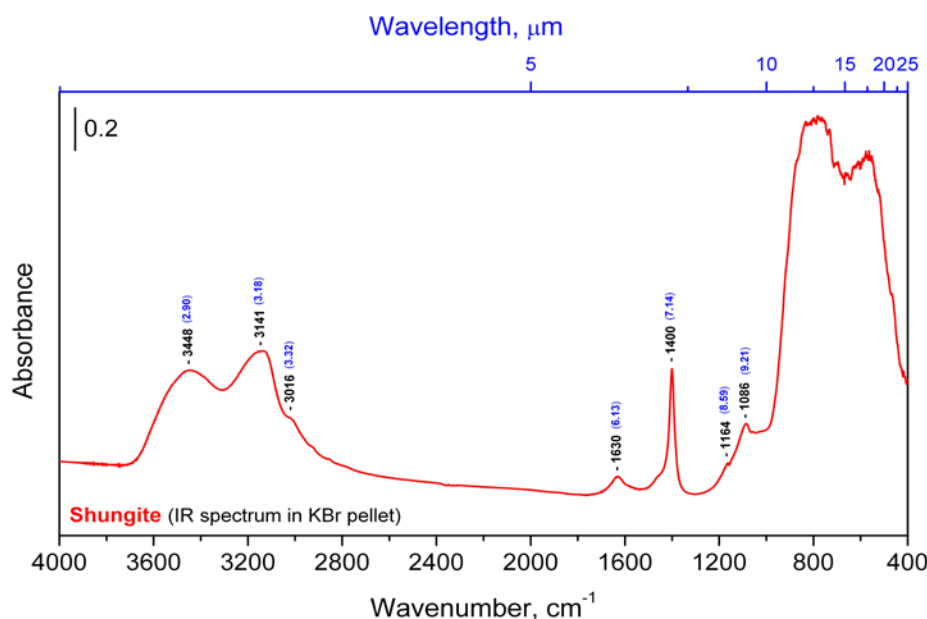
Figure 6. IR-spectrum of shungite in KBr pellet (the spectral range: average IR – 370–7800 cm^{-1}; visible – 2500–8000 cm^{-1}; the permission – 0,5 cm^{-1}; accuracy of wave number – 0,1 cm^{-1} on 2000 cm^{-1})

The average IR region is the most informative and marked as fundamental. In turn, this area is divided into the "fingerprint" region (700–1500 cm^{-1}) and the region of characteristic bands (1500–4000 cm^{-1}).

When interpreting the IR spectra of the organic samples the most informative is the region at 2500–1500 cm^{-1} and the region at 4000–2500 cm^{-1}. Analysis of the first of these allows determine the presence in the sample the unsaturated compounds: C=C, C≡C, C=O, C=N, C≡N, as well as the aromatic and heteroaromatic nucleus. The absorption bands in the region at 4000–2500 cm^{-1} can identify functional groups as O–H, N–H, S–H, as well as various types of carbon-hydrogen C$_{sp3}$–H, C$_{sp2}$–H, C$_{sp}$–H, (O=) C–H-bonds.

The IR spectra of organic compounds can be divided into three main areas (Table 4):

1) 4000–2500 cm^{-1} – a region of stretching vibrations of single bonds X–H: O–H, N–H, C–H, S–H;

2) 2500–1500 cm^{-1} – a region of stretching vibrations of multiple bonds X=Y, X≡Y: C=C, C=O, C=N, C≡C, C≡N;

3) 1500–500 cm^{-1} – a region of stretching vibrations of single bonds X–Y: C–C, C–N, C–O and deformation vibrations of single bonds X–H: C–H, O–H, N–H.

Table 4: Characteristic vibrational frequencies of organic compounds [13]

Groups and types of oscillations	The range of frequencies (cm^{-1}), the intensity of the absorption bands
Covalent C–H bond	
Alkanes C$_{sp3}$–H stretching, ν deformational (I) deformational (II)	2975–2860 (intensive) 1470–1430 (average) 1380–1370 (intensive)
O–CH$_3$ Stretching	2820–2810 (intensive)
CH$_3$Hal (F, Cl, Br, I) stretching, ν	3058–3005 (intensive)

Alkenes C_{sp2}–H stretching, v (=CH$_2$) deformational, δ (–CH=CH$_2$) stretching, v (=CH–) deformational, δ (–CH=CH–) *trans*- *cis*-	3095–3075 (average) 1420–1410 (intensive) 3040–3010 (average) 1310–1295 (average) 970–960 (intensive) ~690 (average)
Aromatic hydrocarbon $C_{arom.}$–H stretching, v deformational, δ	~3030 (intensive) 900–690 (intensive)
Aldehydes stretching, v (I) stretching, v (II)	2900–2820 (not intensive) 2775–2700 (not intensive)
Alkynes C_{sp}–H stretching, v (≡C–H) deformational, δ (–C≡C–H)	~3300 (intensive) 680–610 (intensive)
Covalent bonds X–H	
O–H stretching, v deformational, δ	3650–3590 (average, narrow) 1450–1250 (average, wide)
H-linked bond stretching, v: alcohols, phenols, carbohydrates, carboxylic acids	3550–3200 (intensive, wide) 2700–2500 (wide)
N–H Primary amines and amides (–NH–) stretching, v (2 bands) deformational, δ (amid band II)	3500–3300 (average) 1650–1590 (intensive-average)
Secondary amines and amides (–NH–) stretching, v (I band) deformational, δ (amide band II)	3500–3300 (average) 1650–1550 (not intensive)
Amino acids stretching, v (NH$_3^+$) amino acid band I amino acid band II	1660–1610 (not intensive) 1550–1485 (average)
Imines (+NH–) stretching, v (I band)	3400–3300 (average)
S–H stretching, v	2600–2550 (average)
P–H stretching, v	2440–2350 (average, wide)
Si–H stretching, v	2280–2080 (average)
Covalent bonds X–Y	
C_{sp3}–C_{sp3} stretching, v	1250–1200 (intensive)
C–O stretching, v: primary alcohols secondary alcohols tertiary alcohols phenols	1075–1000 (intensive) 1150–1075 (intensive) 1210–1100 (intensive) 1260–1180 (intensive)

Ethers	
di-alkyl (–CH₂–O–CH₂–)	1150–1060 (very intensive)
aromatic (Ar–O–Ar)	1270–1230 (very intensive)
C–N stretching, v: aliphatic amines primary aromatic amines secondary aromatic amines tertiary aromatic amines aliphatic nitro compounds aromatic nitro compounds	 1220–1020 (average-not intensive) 1340–1250 (intensive) 1350–1280 (intensive) 1360–1310 (intensive) 920–830 (intensive) 860–840 (intensive)
C–Hal stretching, v: C–F C–Cl	 1400–1000 (very intensive) 800–600 (intensive)
C–S stretching, v	 710–570 (not intensive)
C–P stretching, v	 800–700 (shifting)
C–O stretching, v	 870–690 (shifting)
Double covalent bonds X=Y	
C=C stretching, v isolated double bond (C=C) alkenes cumulated double bonds (C=C=C) allenes	 1670–1620 (shifting) ~1950 (intensive) ~1060 (average)
Conjugated double bonds (C=C–C=C or C=C–C=O) alkadienes and enones benzene ring (multiple bands)	 1640–1600 (intensive) ~1600 (shifting) ~1580 (shifting) ~1500 (shifting) ~1450 (shifting)
C=O stretching, v saturated aldehydes, ketones, carboxylic acid esters a-amino acids (COOH) amino acids (COO⁻) unsaturated aldehydes and aromatic ketones amides (amid band I)	 1750–1700 (intensive) 1755–1720 (intensive) 1600–1560 (intensive) 1705–1660 (intensive) 1700–1630 (intensive)
C=N stretching, v	 1690–1630 (shifting)
C=S stretching, v	 1200–1050 (intensive)
N=O stretching, v nitrites (–O–N=O) (2 bands) nitroso (–C–N=O) nitrosamines (–N–N=O)	 1680–1610 (intensive) 1600–1500 (intensive) 1500–1430 (intensive)
C=S stretching, v	 1200–1050 (intensive)

In the sub-region (700–1500 cm^{-1}) are located the absorption bands of the skeleton of the organic molecules comprising C–C-bond, C–O, C–N (for this region are not characteristic oscillations belonging to separate bonds). The nature of the IR-spectrum in this frequency range varies significantly with small differences in the spectra of the organic compounds, as each compound has its unique distinctive set of absorption bands. It can be used to discriminate between the molecules having the same functional group.

In the spectral range of 1500–4000 cm^{-1} are located all fluctuations of the basic functional groups. These groups act as if being isolated and independently of the rest of the molecule, as their absorption frequencies little change at transition from one compound to another. The characteristic may be the bands corresponding to both the stretching and bending vibrations.

Absorption in the region at 1400–1300 cm^{-1} and 700 cm^{-1} is due to deformation oscillations of CH$_3$- and CH$_2$-groups. The stretching vibrations of the terminal C=C bond correspond to the average intensity of the band at 1640 cm^{-1}.

The position band of CH$_2$-group at 800–700 cm^{-1} is dependent on the carbon chain length and is used to detect the organic compounds containing the polymethylene chain.

In the region of 3095–3010; 2975; 3040–3010 cm^{-1} are located stretching vibrations of C–H aromatic, heteroaromatic, small cycles, halogenated alkyl groups.

The main range of characteristic bands of organic compounds changes from 3100–3000 cm^{-1} for H–C-; N–H-; O–H-bonds; 3100–2800 cm^{-1} – for C–H; –CH$_3$-bonds; 3040–3010 cm^{-1} – for =CH-bonds; 1750–1700 cm^{-1} – for C=O bonds; 1690-1630 cm^{-1} – for C=N-bonds; 1670–1620 cm^{-1} – for C=C-bonds; 1420–1410 cm^{-1} – for CH$_2$=CH-bonds; 1310-1295 cm^{-1} – for –CH=CH-bonds; 1250–1200 cm^{-1} – for C$_{sp3}$–C$_{sp3}$-bonds; 1260–1000 cm^{-1} for C–O-bonds; 1220–1020 cm^{-1} – for C–N-bonds; 1400–1300 cm^{-1} – for CH$_2$-bonds; 1640–1600 cm^{-1} – for C=C–C=C or C=C–C=O-bonds; 1060–1950 cm^{-1} for conjugated double C=C=C-bonds (Table 3).

Absorption in the region at 3000–2800 cm^{-1} appears as complex band absorption. The position of bands in this area is preserved in all types of aliphatic hydrocarbons. The intensity of the bands depends on the number of CH$_2$- and CH$_3$-groups in the molecule. The accumulation of CH$_2$-groups increases the intensity of the absorption band of 3000–2800 cm^{-1}, whereas the intensity of the band of the CH$_3$–group changes little. This property is used for quantitative analysis of hydrocarbons. Thus, the carbonaceous composition of shungite is complex; this mineral contains in its composition many functional groups of organic compounds with different types of bonds, which is due to its complex organic composition.

Evaluation of the mathematical model of interaction of shungite and zeolite with water

Other method for obtaining the information about the average energy of hydrogen bonds in an aqueous sample is measuring the spectrum of the water state. It was established experimentally that at evaporation of water droplet the contact angle θ decreases discretely to zero, whereas the diameter of the droplet changes insignificantly [21]. By measuring this angle within a regular time intervals a functional dependence f(θ) can be determined, which is designated by the spectrum of the water state (SWS) [22–24]. For practical purposes by registering the SWS it is possible to obtain information about the averaged energy of hydrogen bonds in an aqueous sample. For this purpose the model of W. Luck is used, which consider water as an associated liquid, consisted of O–H...O–H groups [25]. The major part of these groups is designated by the energy of hydrogen bonds (-E), while the others are free (E = 0). The energy distribution function f(E) is measured in electron-volts (eV^{-1}) and may be varied under the influence of various external factors on water as temperature and pressure.

For calculation of the function *f(E)* the experimental dependence between the water surface tension measured by the wetting angle (θ) and the energy of hydrogen bonds (E) in an aqueous sample is used:

$$f(E) = \frac{14{,}33 f(\theta)}{[1-(1+bE)^2]^2},$$

where $b = 14,33$ eV^{-1}; $\theta = arcos(-1 - b\,E)$

The energy of hydrogen bonds (E) measured in electron-volts (eV) is designated as the spectrum of energy distribution. This spectrum is characterized by non-equilibrium process of water droplets evaporation, thus the term "non-equilibrium energy spectrum of water" (NES) is applied.

The difference $\Delta f(E) = f\,(E_{\text{samples of water}}) - f\,(E_{\text{control sample of water}})$

– is designated the "differential non-equilibrium energy spectrum of water" (DNES).

The DNES is a measure of changes in the structure of water as a result of external factors, because the energy of hydrogen bonds in water samples differ due to the different number of hydrogen bonds in water samples, which may result from the fact that different waters have different structures and composition and various intermolecular interactions – the various associative elements etc. The redistribution of H_2O molecules in water samples according to the energy is a statistical process of dynamics.

It was studied the distribution of local extremums in water solutions of of shungite and zeolite regarding the energies of hydrogen bonds. The average energy ($\Delta E_{H...O}$) of hydrogen H...O-bonds among individual H_2O molecules was calculated for the water solutions of of shungite and zeolite by NES- and DNES-methods. The research with the NES method of water drops, received after their being exposed for 3 days with shungite and zeolite in deionized water, may also give valuable information on the possible number of hydrogen H...O-bonds as a percent (%) of individual H_2O molecules with different values of distribution of energies of hydrogen bonds (Table 5). These distributions are basically connected with the re-structuring of H_2O molecules with the same energies.

Table 5: Characteristics of spectra of water after 3 days infusion with shungite and zeolite, obtained by NES-method

-E(eV) x-axis	Shungite, % [(-E$_{value}$)/ (-E$_{total\ value}$)]	Zeolite, % [(-E$_{value}$)/ (-E$_{total\ value}$)]	-E(eV) x-axis	Shungite, % [(-E$_{value}$)/ (-E$_{value}$)]	Zeolite, % [(-E$_{value}$)/ (-E$_{total\ value}$)]
0,0937	2,85	6,3	0,1187	0	12,4
0,0962	8,8	6,3	0,1212	5,9	6,3
0,0987	5,9	0	0,1237	0	0
0,1012	11,8	12,4	0,1262	0	0
0,1037	11,8	6,3	0,1287	0	18,7
0,1062	0	6,3	0,1312	8,8	6,3
0,1087	0	0	0,1337	2,85	0
0,1112	5,9	0	0,1362	0	0
0,1137	11,8	0	0,1387	11,8	2,4
0,1162	11,8	6,3	–	–	–

The distribution [%, (-E$_{value}$)/(-E$_{total\ value}$] of H_2O molecules in water solution of shungite/zeolite according to energies of hydrogen bonds and local extremums in NES and DNES spectra of water solutions of of shungite and zeolite is shown in Figure 6 and Table 6. The average energy ($\Delta E_{H...O}$) of hydrogen H...O-bonds among individual molecules H_2O after the treatment of shungite and zeolite with water was measured to be at -0,1137 eV for shungite and -0,1174 eV for zeolite. The result for the control sample (deionized water) was -0,1162 eV. The results obtained with the NES method were recalculated with the DNES method. Thus, the result for shungite measured with the DNES method was +0,0025±0,0011 eV and -1,2±0,0011 eV for zeolite. This difference may indicate on the different mechanisms of interaction of these minerals with water, but also may has been the result of the different composition and the structure of these two minerals, resulting in different behavior while the interaction with water.
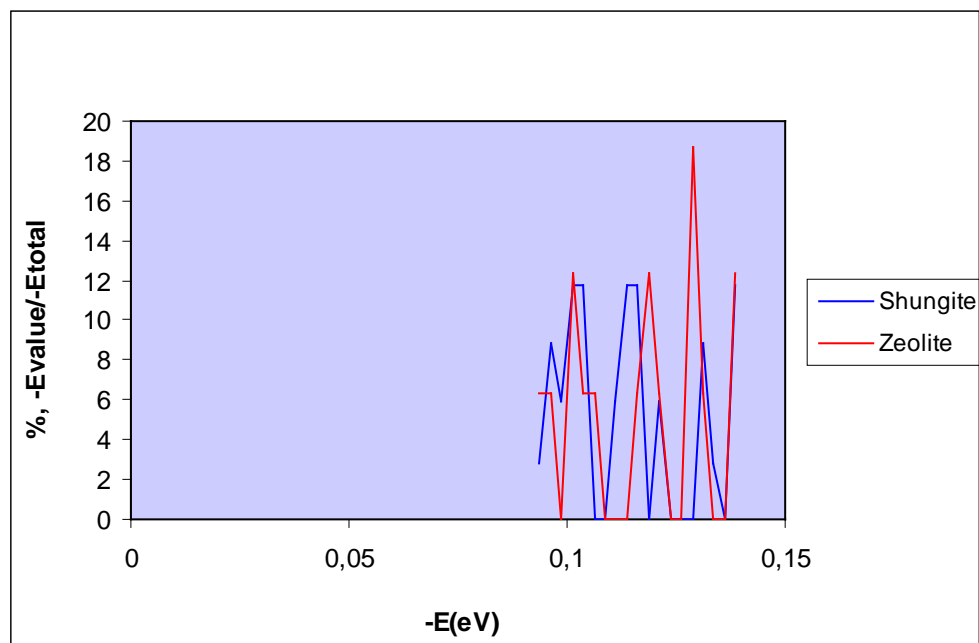
Figure 6. The distribution [%, $(-E_{value})/(-E_{total\ value})$] of water molecules in water solution of shungite/zeolite according to energies of hydrogen bonds ($-E_{value}$) to a total result of hydrogen bonds energy

Table 6: Distribution of energies of hydrogen bonds and the local extremums in NES and DNES spectra of water solutions of shungite and zeolite

-E(eV) x-axis	NES Shungite	NES Zeolite y-axis (eV⁻¹)	NES Control sample y-axis (eV⁻¹)	DNES Shungite y-axis (eV⁻¹)	DNES Zeolite y-axis (eV⁻¹)	-E(eV) x-axis	NES Shungite y-axis (eV⁻¹)	NES Zeolite y-axis (eV⁻¹)	NES Control Sample y-axis (eV⁻¹)	DNES Shungite y-axis (eV⁻¹)	DNES Zeolite y-axis (eV⁻¹)
0,0937	11,8	25,0	0	11,8	25,0	0,1187	0	50,0	30,8	-30,8	19,8
0,0962	35,3	25,0	30,8	4,5	-5,8	0,1212	23,5	25,0	30,8	7,3	5,8
0,0987	23,5	0	0	23,5	0	0,1237	0	0	0	0	0
0,1012	47,1	50,0	0	47,1	50,0	0,1262	0	0	30,8	-30,8	-30,8
0,1037	47,1	25,0	30,8	16,3	-5,8	0,1287	0	75,0	0	0	75,0
0,1062	0	25,0	0	0	25,0	0,1312	35,3	25,0	0	35,3	25,0
0,1087	0	0	76,9	-76,9	-76,9	0,1337	11,8	0	30,8	-19,0	-30,8
0,1112	23,5	0	15,4	8,1	-15,4	0,1362	0	0	15,0	-15,0	-15,0
0,1137	47,1	0	30,8	16,3	-30,8	0,1387	47,1	50,0	15,0	32,1	35,0
0,1162	47,1	25,0	61,5	-14,4	-36,5	–	–	–	–	–	–

The results also suggest the restructuring of the energy values among the individual H_2O molecules with a statistically reliable increase of local maximums in DNES-spectra. For the value -0,1387 eV there was a local maximum with positive values for shungite and zeolite. In this regard it should be noted that A. Antonov early demonstrated that in the aqueous suspension of tumor cells there was detected a decrease of local maximums; DNES-spectra of aqueous solution containing Ca^{2+} have a local minimum of energy at -0,1 eV and a local maximum at -0,11 eV. The interesting fact is that due to the present of calcium in shungite, the aqueous solution of shungite has a local minimum of energy at -0,0987 eV and a local maximum at -0,1137 eV that closely corresponds with the DNES-spectrum of aqueous solution containing Ca^{2+}. Thus, by the analyzing the NES- and DNES-spectra of aqueous solutions of shungite and zeolite in water it is possible to evaluate the base of the mathematical model of interaction of these minerals with water, judging by the

structural properties, the energies of of hydrogen H...O-bonds and the distribution the individual H_2O molecules in samples with different values of energies.

Table 7 shows the local extremums in spectra of different samples of mountain water, as well as ions of Ca^{2+}, Na^+, Mg^{2+}, Fe^{2+}, SO_4^{2-} and pH values. For all these types of water is applied a new parameter in Table 6 – the local extremum, measured at -0,1362...-0,1387 eV. Its value in the NES-spectrum is measured as the function of distribution of individual H_2O molecules in water samples according to energy f(E) of hydrogen bonds. The function of distribution of individual H_2O molecules according to energy f(E) of hydrogen bonds for tap water from Teteven (Bulgaria) is measured up at 23,8±1,2 eV^{-1}.

Table 7: The composition of mountain water sources from Teteven (Bulgaria), their pH values and local extremums in spectra after exposition with shungite

Water sources	Ca^{2+}	Na^+	Mg^{2+}	Fe^{2+}	SO_4^{2-}	pH	Local extremum* at (-0,1362...-0,1387 eV) (1)	Local extremum* with shungite (-0,1362...-0,1387 eV) (2)	Difference between (2) and (1)
	mg/dm³ norm (<150)	mg/dm³ norm (<200)	mg/dm³ norm (<80)	mg/dm³ norm (<200)	mg/dm³ norm (<250)	norm (6,5–9,5)	eV^{-1} norm (>24,1)	eV^{-1} norm (>24,1)	eV^{-1} norm (>24,1)
1. Deionized water (control)	–	–	–	–	–	–	15,4 ±0,8	47,1 ±2,8	31,7 ±1,6
2. Klindiovo	89,9 ±9,0	4,1 ±0,4	6,98 ±0,7	40,2 ±4,0	17,7 ±1,8	8,0 ±0,1	44,4 ±2,2	63,2 ±3,2	18,6 ±0,9
3. Gorna cheshma	103,6 ±10,4	4,2 ±0,4	15,5 ±1,6	9,6 ±0,96	89,9 ±9,0	7,3 ±0,1	51,6 ±2,6	80,0 ±4,0	28,4 ±1,4
4. Dolna cheshma	94,4 ±0,94	2,5 ±0,3	12,10 ±1,21	9,0 ±0,9	15,99 ±1,6	7,9 ±0,1	34,2 ±1,7	51,6 ±2,6	17,4 ±0,9
5. Sonda	113,6 ±11,4	7,3 ±0,7	15,99 ±1,60	5,00 ±0,5	57,2 ±5,7	7,3 ±0,1	54,4 ±2,7	70,6 ±3,5	16,2 ±0,8
6. Ignatov izvor	40,44 ±4,04	0,62 ±0,12	2,46 ±0,25	13,0 ±1,4	17,9 ±1,8	6,82 ±0,1	48,0 ±2,4	85,7 ±4,3	37,7 ±1,9
7. Gechovoto	66,0 ±6,0	1,46 ±0,15	2,1 ±0,2	11,4 ±1,1	15,9 ±1,6	7,94 ±0,1	41,7 ±2,1	84,2 ±4,2	42,5 ±2,1

*Notes: The function of distribution of individual H_2O molecules according to energy f(E) of hydrogen bonds for tap water in Teteven (Bulgaria) is 23,8±1,2 eV^{-1}; results refer to the influence of shungite on different sources of mountain water according to energy f(E) of hydrogen bonds.

We have obtained new data for the influence of shungite on NES- and DNES-spectra of different mountain water sources and characteristics of spectra (Table 7). The peculiarities consist in the values of the local extremum measured at -0,1362...-0,1387 eV. It was detected the tendency of the increasing of local extremums in aqueous solution of shungite in water regarding the same mountain water samples as regard to the control sample. The distribution of local extremums detected at -0,1362...-0,1387 eV has an inversely character dependent for the ion content in water for the difference at -0,1362...-0,1387 eV of the shungite solution in mountain water and the same water as a control sample. These results suggest about the different mechanisms of interactions of these minerals with water with a statistically reliable increase of local maximums in DNES-spectra. The data obtained are very promising and further need to be scrutinized seriously. The research will be continued in future with new experiments.

Conclusion

The fullerene-containing natural mineral shungite and microporous crystalline aluminosilicate mineral zeolite have a complex multicomponent composition. The efficiency of using and studying these two natural minerals is stipulated by the high range of valuable properties (absorption, catalytic, antioxidant, regenerative), high environmental safety and relatively low cost of filters based on shungite and zeolite as well as existence of the extensive domestic raw material

base of shungite and zeolite deposits. All these factors contribute to the further studies. As the result of our studies the base of the mathematical model describing the interaction of these two minerals with water was established. It allows understand better, how these minerals interact with H_2O molecules in water solutions in order to explain the physical-chemical and adsorption properties of these minerals.

Aknowlegements

References:

1. Khavari-Khorasani G. The nature of carbonaceous matter in the Karelian shungite / G. Khavari-Khorasani, D.G. Murchison // *Chem. Geol.* 1979. V. 26. P. 165–82.

2. Mosin O.V. The structure and composition of natural carbonaceous fullerene containing mineral shungite / O.V. Mosin, I. Ignatov // *International Journal of Advanced Scientific and Technical Research.* 2013. V. 6, № 11–12. P. 9–21.

3. Gorshteyn A.E. Adsorption properties of shungites / A.E. Gorshteyn, N.Y. Baron, M.L. Syrkina // *Izv. Vysshykh Uchebn. Zaved. Khimia i Khim. Technol.* 1979. V. 22, № 6. P. 711–715 [in Russian].

4. Cascarini de Torre L.E. Characterization of shungite by physical adsorption of gases / L.E. Cascarini de Torre, A.E. Fertitta, E.S. Flores, J.L. Llanos, E.J. Bottani // *J. Argent. Chem. Soc.* 2004. V. 92, № 4–6. P. 51–58.

5. Podchaynov S.F. Mineral zeolite – a multiplier of useful properties shungite. Shungites and human safety, in *Proceedings of the First All-Russian scientific-practical conference* (3–5 October 2006) / Ed. J.K Kalinin. – Petrozavodsk: Karelian Research Centre of Russian Academy of Sciences. 2007. P. 6–74 [in Russian].

6. Volkova I.B. / I.B. Volkova, M.V. Bogdanov // Petrology and genesis of the Karelian shungite-high rank coal. *Int. J. Coal Geol.* 1986. V. 6. P. 369–79.

7. Panayotova M. Kinetics of heavy metal ions removal by use of natural zeolite / M. Panayotova, B. Velikov // *Journal of Environmental Science and Health.* 2002. V. 37, № 2. P. 139–147.

8. Parfen'eva L.S. Electrical conductivity of shungite carbon / L.S. Parfen'eva // *Solid State Physics.* 1994. V. 36, № 1. P. 234–236.

9. Kasatochkin V.I. Submikroporous structure of shungites / V.I. Kasatochkin, V.M. Elizen, V.M. Melnichenko, I.M. Yurkovsky, V.S. Samoilov // *Solid Fuel Chemistry.* 1978. № 3. P. 17–21.

10. Khadartsev A.A. Shungites in medical technologies / A.A. Khadartsev, I.S. Tuktamyshev // *Vestnik Novih Medicinskih Technologii.* 2002. V. 9, № 2. P. 83–86 [in Russian].

11. Kovalevski V.V. Structure of shungite carbon / V.V. Kovalevski // *Natural Graphitization Chemistry.* 1994. V. 39. P. 28–32.

12. Mosin O.V. Composition and structural properties of fullerene analogous mineral shungate / O.V. Mosin, I. Ignatov I // *Journal of Nano and Microsyctem Technique.* 2013. V. 1. P. 32–40 [in Russian].

13. Golubev E.A. *Local supramolecular structures shungite carbon* / E.A. Golubev // in Proceedings of the Int. Symp. "Carbon-formation in geological history". – Petrozavodsk: Publishing House of the Karelian Research Center, Russian Academy of Sciences. 2000. P. 106–110 [in Russian].

14. Kovalevsky V.V. Comparison of carbon in shungite rocks to other natural carbons: an X-ray and TEM study / V.V. Kovalevski, P.R. Buseckb, J.M. Cowley // *Carbon.* 2001. V. 39. P. 243–256.

15. Jushkin N.P. Globular supramolecular structure shungite: data scanning tunneling microscopy / N.P. Jushkin // *Reports. Acad. Science USSR.* 1994. V. 337, № 6. P. 800–803 [in Russian].

16. Reznikov V.A. Shungite amorphous carbon – the natural environment of fullerene / V.A. Reznikov, Y.S. Polehovsky // *Technical Physics Letters.* 2000. V. 26, № 15. P. 689–693.

17. Kalinin Yu.K. The structure of the shungite carbon and possibility of the presence of fullerenes / Yu.K. Kalinin // *Solid State Chemistry.* 2002. № 1. P. 20–28.

18. Mosin O.V. The Composition and structural properties of fullerene natural mineral shungite / O.V. Mosin, I. Ignatov // *Nanoengineering*. 2012. V. 18, № 12. P. 17–24 [in Russian].

19. Pleshakov V. Computer models of icosahedral carbon nanostructures (shungite) / V. Pleshakov // *J. Appl. Cryst.* 2014. V. 47. P. 539–543.

20. Ignatov I. The structure and composition of carbonaceous fullerene containing mineral shungite and microporos crystalline alumosilicate mineral zeolite / I. Ignatov, O.V. Mosin // *Nanotechnology Research and Practice*. 2014. V.1, № 1. P. 30–42.

21. Antonov A. *Research of the nonequilibrium processes in the area in allocated systems* / A. Antonov. Diss. thesis doctor of physical sciences. – Sofia: Blagoevgrad. 2005. P. 1–255.

22. Ignatov I. Structural mathematical models describing water clusters / I. Ignatov, O.V. Mosin // *Journal of Mathematical Theory and Modeling*. 2013. V. 3, № 11. P. 72–87.

23. Ignatov I. *Energy Biomedicine* / Ed. I. Ignatov. – Sofia: Gea-Libris. 2005. P. 1–88.

24. Ignatov I. Water in human body is informational bearer about longevity / I. Ignatov // in *Conference on the Physics, Chemistry and Biology of Water.* – Vermont Photonics. USA, 2012. P. 137.

25. Luck W. Infared investigation of water structure in desalination membranes / W. Luck, D. Schiöberg, S. Ulrich // *J. Chem. Soc. Faraday Trans.* 1980. V. 2, № 76. P. 136–147.

Методы неравновесного энергетического спектра и дифференциального неравновесного энергетического спектра в изучении взаимодействия углеродсодержащего минерала шунгита и алюмосиликатного минерала цеолита с водой

[1] Игнат Игнатов
[2] Олег Викторович Мосин

[1] Научно-исследовательский центр медицинской биофизики (РИЦ МБ), Болгария
Профессор, доктор наук Европейской академии естественных наук (ФРГ), директор НИЦ МБ.
1111, София, ул. Н. Коперника, 32/6
E-mail: mbioph@dir.bg
[2] Московский государственный университет прикладной биотехнологии, Российская Федерация
Старший научный сотрудник кафедры биотехнологии, канд. хим. наук.
103316, Москва, ул. Талалихина, 33
E-mail: mosin-oleg@yandex.ru

Аннотация. Построена математическая модель взаимодействия с водой аморфного, некристаллизирующегося, фуллереноподобного углеродсодержащего минерала шунгита (Зажогинское месторждение, Карелия, РФ) и микропористого кристаллического алюмосиликатного минерала цеолита (Мост, Болгария). Приведены данные о наноструктуре, а также о составе и химико-физические свойства этих минералов, полученные с помощью элементного анализа, сканирующей электронной микроскопии (СЭМ) и ИК-спектроскопии. Для построения математической модели взаимодействия этих минералов с водой использовали методы неравновесного энергетического спектра (НЭС) и дифференциально-неравновесного энергетического спектра (ДНЭС). Измерены величины средней энергии ($\Delta E_{H...O}$) водородных H...O-связей между молекулами H_2O после обработки шунгита и цеолита водой, составляющие -0,1137 эВ для шунгита и -0,1174 эВ для цеолита. Расчет $\Delta E_{H...O}$ для шунгита с использованием ДНЭС-метода составляет +0,0025±0,0011 эВ, а для цеолита -1,2±0,0011 эВ. Показана закономерность изменения энергии водородных связей между молекулами H_2O при обработке воды шунгитом и цеолитом со статистическим повышением локальных максимумов в ДНЭС-спектрах воды.

Ключевые слова: шунгит, цеолит, наноструктура, фуллерены, ИК, НЭС, ДНЭС